J Mater Sci (2011) 46:5085–5089
DOI 10.1007/s10853-011-5435-6

Ultra-sharp pointed tip Si nanowires produced by very high frequency plasma enhanced chemical vapor deposition via VLS mechanism

Habib Hamidinezhad · Yussof Wahab · Zulkafli Othaman

Received: 20 January 2011 / Accepted: 2 March 2011 / Published online: 11 March 2011

Abstract Needle-like silicon nanowires have been grown using gold colloid as the catalyst and silane (SiH_4) as the precursor by very high frequency plasma enhanced chemical vapor deposition (VHF-PECVD). Si nanowires produced by this method were unique with sharpness below 3 nm. High resolution transmission electron microscopy (HRTEM) and X-ray diffraction technique (XRD) confirmed the single crystalline growth of the Si nanowires with (111) crystalline structure. Raman spectroscopy also has revealed the presence of crystalline Si in the grown Si nanowire body. In this research, presence of a gold nanoparticle on tip of the nanowires proved vapor–liquid–solid growth mechanism.

Introduction

One-dimensional nanostructures have attracted extensive interest due to their potential uses in nanoelectronic and optoelectronic devices and fundamental importance for the study of size-dependent chemical and physical phenomena [1–3]. Among these one-dimensional nanomaterials, silicon nanowires (SiNWs) have attracted much attention due to their fitness with conventional silicon-based integrated circuit (IC) technology. SiNWs are particularly favorable to be used as building block to fabricate nanoscale devices such as nanotransistors [4], metal–oxide–semiconductor field effect transistors (MOSFETs) [5], sensors [6], logic device [7], and solar cells [8]. Small diameter SiNWs are fronted as attractive nanomaterials due to their quantum size effect for future devices. Theoretical calculations indicate that essential quantum size effects will happen for a SiNW with diameter of below 10 nm [9].

In the past few years, several researchers have reported the synthesis of SiNWs using various methods, including laser ablation [10], supercritical fluid solution-phase [11], thermal vapor deposition [12], rapid chemical etching technique [13], chemical vapor deposition (CVD) [14], and plasma enhanced chemical vapor deposition (PECVD) [15]. Among chemical techniques PECVD is one of the most advanced techniques. The PECVD technique is a directional deposition method. In PECVD process a gas such as silane and the subsequent metal catalyst moderates growth of SiNWs. This involves a mechanism that is famous as vapor–liquid–solid (VLS) and was first proposed by Wagner and Ellis [16]. The VLS fabrication mechanism is the most successful synthesis method for fabrication single crystalline Si nanowires with high production yields [17]. In the VLS mechanism, a metal catalyst as Au is deposited onto a substrate as silicon. This catalyst can be thin layers or nanoparticles. Usually Au nanoparticles catalysts have a remarkable capacity to control SiNW sizes.

In this present research, very high frequency plasma enhanced chemical vapor deposition (VHF-PECVD) was used for growth of Au-catalyzed SiNWs on Si substrate. Theoretical and experimental consideration indicates that the VHF-PECVD has advantages such as high deposition speed, good quality, higher electron density, lower plasma potential and photovoltaic performance due to reduced ion bombardment compared to the conventional RF (13.56 MHz) PECVD [18, 19]. In this technique nanowires can be grown with good crystallinity and high growth rate at lower substrate temperature compared to other methods. The morphology of Si nanowires was

---

H. Hamidinezhad (✉) · Y. Wahab · Z. Othaman
Ibnu Sina Institute for Fundamental Science Studies (IIS), UTM, Skudai 81310, Johor, Malaysia
e-mail: habib_hamidinezhad@yahoo.com

different from previously grown Si nanowires by conventional VLS methods [20, 21]. Our Si nanowires are needle-like with a unique sharpness below 3 nm. These nanoneedles are sharper than nanoneedles fabricated in last report [22].

Experiments

SiNWs were synthesized with an Au catalyst on a Si (111) wafer by the VHF-PECVD method in vacuum. In this study, Si wafer was coated with 30 nm sized gold colloid particle solution as a catalyst. The size of Au catalytic plays an important role on diameter of SiNWs in VLS mechanism because it takes a place at droplet interface [23]. To obtain small diameter catalysts, the Au-coated substrate was heated at the temperature of 500 °C during 5 min. For the synthesis of the SiNWs, pure SiH_4 (99.9995%) gas as the Si source with 10 sccm was introduced to VHF-PECVD vacuum reactor at the pressure of 77 mtorr for 10 min. The power of RF plasma and frequency were 15 W and 150 MHz respectively. During the deposition, the substrate temperature has been held at 370 °C. The as-grown SiNWs were then analyzed using a field emission scanning electron microscope (FESEM, JEOL, JSM-6701F) and high resolution transmission electron microscopy (HRTEM, JEOL, JEM-2100). The elemental composition of the ultra-sharped SiNWs and their crystal phase were analyzed through an X-ray diffraction technique (XRD), with Cu Kα radiation and an energy dispersive X-ray spectrometer (EDX). Raman spectroscopy was performed using a spectrum GX (NIR, FT-Raman) system with an Nd crystal laser source and 1 µm spot size.

Results and discussion

Figure 1 shows the FESEM image of SiNWs synthesized on Si (111) substrates using a gold-catalyzed VHF-PECVD method under the experimental conditions described in the figure caption. According to figure, a population of needle-like ultra-sharp pointed nanowires with lengths ranging from 4 to 5 µm was grown on Si wafer. Adjusting the RF power and the temperature leads to the controlled growth of ultra-sharp pointed SiNWs, as seen in Fig. 1.

Figure 2 shows the EDX spectra of the nanowires. EDX shows that these nanowires are composed mainly of Si and Au (93.37 and 6.62 at.%, respectively).

Figure 3 displays low magnification TEM and HRTEM images of uppermost part of SiNWs generated in this research. The low magnified TEM (Fig. 3a) provides further information regarding the structure of grown SiNWs.

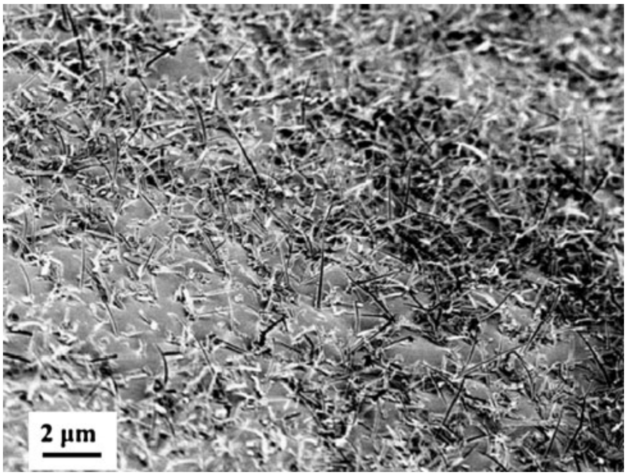

Fig. 1 FESEM image of ultra-sharp pointed silicon nanowires synthesized with gold colloid as catalyst on Si (111)-oriented using VHF-PECVD method. The nanowires were grown for 15 min at temperature of 370 °C and RF power of 15 W

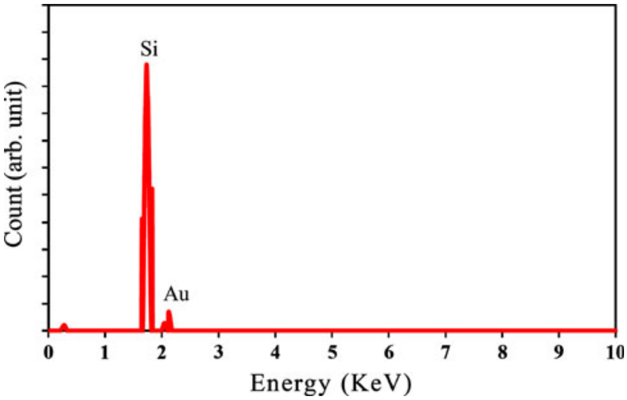

Fig. 2 The EDX spectra of the ultra-sharp pointed SiNWs

From this image, it can be seen that the wire has needle-like structure with ultra-sharp pointed tip. This result corresponds to the results obtained with the FESSEM image. In Fig. 3b a very small Au catalyst particle is also observed at the tips of ultra-sharp SiNWs. The morphology verifies that the SiNWs were obtained by Au-catalyzed VLS growth mechanism. Before growth of nanowires, the size of gold colloid solution deposited on silicon substrate was 30 nm. However, the Au catalyst size on tip of nanowires at the end of synthesis decreased 10 to 15 times of the nominal size at the beginning. Figure 3c shows the HRTEM image of SiNW grown in this experiment. The structure is further confirmed by HRTEM characterization of Si nanowire. HRTEM image reveals that each nanowire consists of single crystalline structure. According to the HRTEM measurement and the following calculation by the software of the HRTEM digital micrograph, the interplanar spacing of crystals is about 0.314 nm, matching well

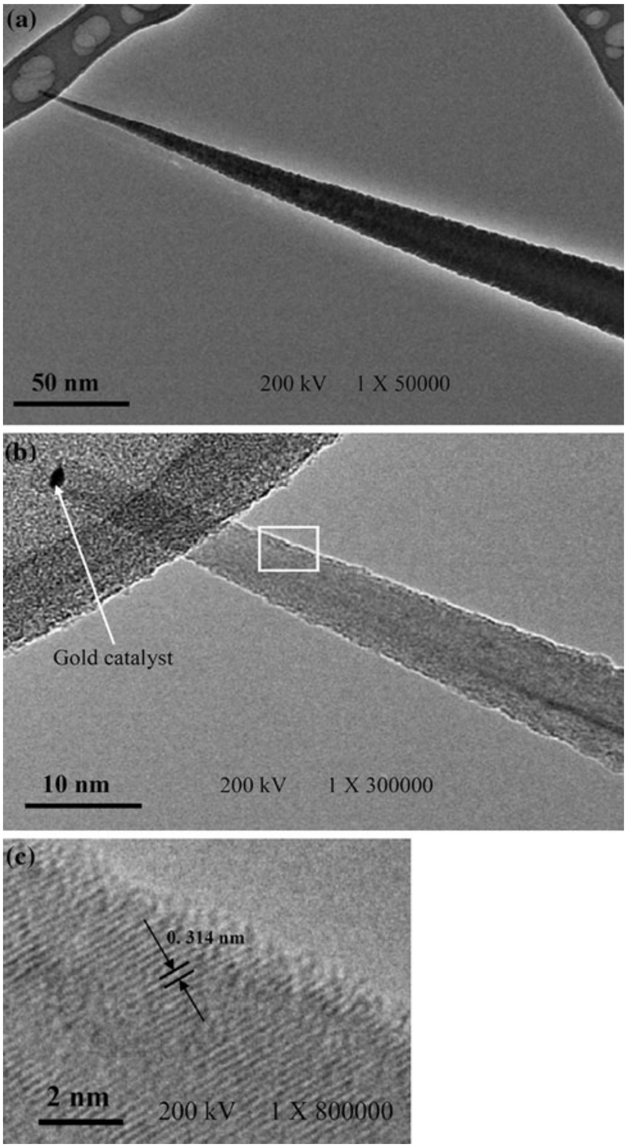

Fig. 3 **a** The low magnified TEM grown SiNW reveals that the wire is needle-like structure with ultra-sharp pointed tip. **b** A very small Au catalyst particle (*black spot*) placed at the tips of the ultra-sharp SiNW. The size of Au particle and tip of wire are 1.85 and 2.408 nm, respectively. **c** The HRTEM image of a section of SiNW shown in *white box* drowns in Fig. 3**a** reveals that each nanowire consists of crystalline structure with interplanar spacing of crystals about 0.314 nm, matching well with the ⟨1 1 1⟩ growth direction

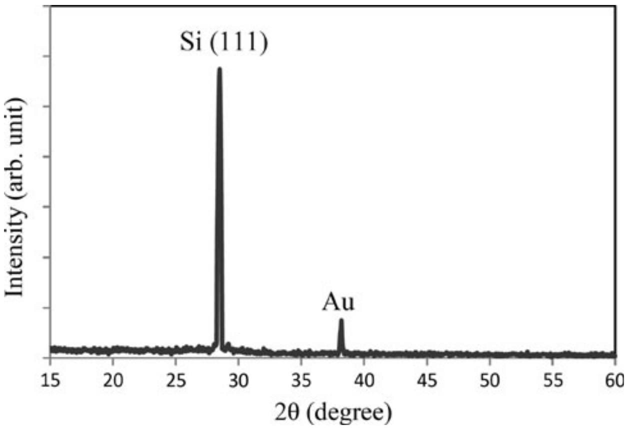

Fig. 4 The XRD spectrum of the ultra-sharp pointed SiNWs grown on the Si substrate

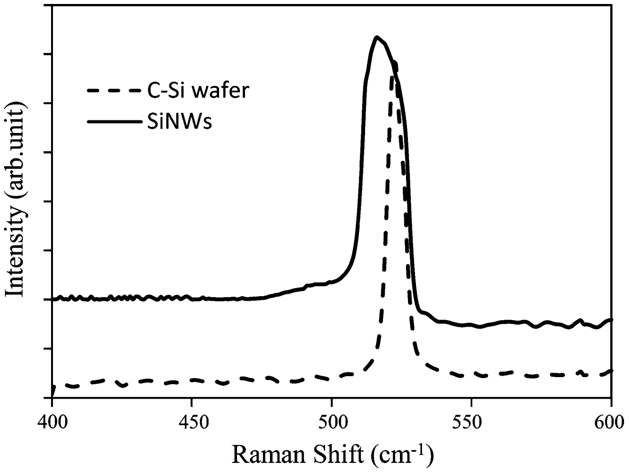

Fig. 5 Raman spectrum of a single crystalline of ultra-sharp pointed SiNW (*solid line*) and silicon wafer (*dashed line*) at room temperature. The ultra-sharp pointed SiNW has an asymmetry peak centered at 516 cm^{-1}. The sharp peak at 522 cm^{-1} corresponds to crystalline Si substrate

with the {1 1 1} plane of silicon and the growth of the nanowire is along the ⟨1 1 1⟩ direction.

Figure 4 shows the XRD spectrum of the ultra-sharp pointed SiNWs grown on the Si substrate, which displays high-intensity peak of the Si (1 1 1) indicating that the SiNWs were the well single crystalline structure. The spectrum also exhibited the growth direction of the SiNWs was ⟨111⟩ orientation, which is consistent to the results of the HRTEM (Fig. 3). Calculated from the inter-planar spacing of the most intense (111) peak ($d = 0.314$ nm), the lattice parameter of the SiNWs was obtained as $a = 0.5452$ nm; which is larger than the standard value $a = 0.5430$ nm for bulk silicon. This reveals that there is a slight lattice expansion and distortion in the SiNWs structure. There is not any trace of oxygen peaks in the XRD spectrum. Au peak was also detected because the gold nanoparticles as catalyst were located on the top of tapered SiNWs as shown in HRTEM images.

Most of the Si nanowires produced by Au catalyst have had uniform diameters of higher than 10 nm [20, 24]. The tip radius of produced nanocone by other researchers via VLS mechanism also was in range of 10–200 nm [22, 25, 26]. Thus, our ultra-sharp pointed Si nanowires with an unprecedented sharpness of below 3 nm are unique in the category of Au-catalyzed grown Si nanowires via VLS mechanism using PECVD method.

Figure 5 shows the Raman spectra of the as-grown SiNWs (solid line) and a single crystalline Si wafer (dashed line). Raman spectroscopy is very sensitive to the lattice structure and the crystal symmetry. The Peak energy, the peak width, and the symmetry in Raman Spectra change with reduction of the Si nanowires size [27]. As seen in Fig. 5 the as-grown SiNWs has an asymmetry Raman peak centered at 516 cm^{-1} where this peak is remarked to be the first-order transverse optical photon mode (TO). The high symmetric peak centered at 522 cm^{-1} is related to bulk crystalline silicon. Important downshift of the asymmetrical TO peak shown from 522 cm^{-1} of bulk silicon to 516 cm^{-1} of SiNWs is due to the diameter decrease of the SiNWs [28]. Here, size confinement or nanoscale size of wires is the reason of asymmetry and broadened width of peak in spectrum. This is a sign of phonon confinement [29]. Raman spectroscopy taken from SiNWs reveals that their structure is crystalline. This is consistent with the HRTEM analysis in Fig. 3c.

A comparison between VHF-PECVD method with those of some other researchers for the growth of Si nanoneedles and nanowires is shown in Table 1. According to the table, the tip diameter and the growth temperature of nanowires produced by VHF-PECVD method are remarkably lower than those of the nanoneedles and nanowires grown using other systems. Furthermore, grown nanoneedles using VHF-PECVD method in this research have only single crystalline structure, while others results show nanoneedles and nanowires having crystalline core and amorphous shell structures.

It should be noted that in the present work, the growth rate of Si nanowires, around 500 nm/min, was approached during 10 min deposition. This value is significantly higher than the usual growth rates (12–50 nm/min) of Si nanowires grown by classical CVD, low pressure CVD (LPCVD) and conventional medium frequency of 13.56 MHz PECVD methods [15, 24, 30, 31]. This fast growth rate is probably due to plasma power which causes high decomposition of the $\mathrm{SiH_4}$ gas.

The existence of Au peak in spectra confirmed that the Au catalyst-assisted VLS mechanism was occurred during the growth process. The VLS mechanism correctly describes the gold-catalyzed CVD growth of nanowires. In this mechanism, the silane ($\mathrm{SiH_4}$) molecules at first decompose onto the surface of gold catalyst nanoparticles in the form of silicon. Then, the silicon atoms dissolve into the liquid gold particles result in formation of Au–Si alloy. The continuing adsorption of the Si in Au–Si liquid droplets leads to supersaturating of the alloy which brings about growth of a solid silicon core in the bottom of the droplet. The Au–Si droplet remains at the top of the solid silicon and can accepts more silicon atom from the source. As a result, the solid silicon grows in the liquid-solid interface leading to growing nanowire. Therefore, the VLS reaction includes three distinct stages: (a) diffusion of silicon atoms from the vapour source to the vapour/Au–Si droplet interface; (b) diffusion of silicon atoms into the liquid droplet; (c) precipitation of Si atoms at the droplet/nanowire interface. The decomposition of $\mathrm{SiH_4}$ gas is a thermally activated process in which the activation energy of the CVD grown SiNWs with an Au-catalyzed was found in compliance with the activation energy of $\mathrm{SiH_4}$ decomposition [32]. With utilizing the plasma activation to CVD system for growth of SiNWs, the VLS mechanism is no longer valid, since the plasma deposition is a non-equilibrium process thermodynamically. Moreover, VHF-PECVD causes $\mathrm{SiH_4}$ to pre-dissociate to an ionized gas. Accordingly, the silicon atoms have a greater diffusion and adsorption potential in VHF-PECVD than in CVD. As the $\mathrm{SiH_4}$ molecules are dissociated in the plasma, the growth process is not limited by $\mathrm{SiH_4}$ decomposition rate as in CVD and other factors start playing a role.

The other main effect of the very high frequency plasma enhanced CVD system is the non-catalyzed Si sidewall deposition. This type of deposition causes tapering of Si nanowires in VHF-PECVD, where it allows production of Si nanoneedles with ultra-sharped tip. As shown in HRTEM image (Fig. 3c), the Si nanoneedle consists of the crystalline Si structure. The VHF-PECVD growth conditions promoted the growth of crystalline Si layers on the surface of the nanoneedle sidewall without gold catalytic nanoparticles during the growth of nanowire.

Synthesizing needle-like SiNWs below 3 nm in tip will open up the door to fabricate worthwhile devices where quantum effects play a significant role. These ultra-sharp nanoneedles can be used as tips of special microscopes, for

Table 1 Characteristic of nanowires and nanoneedles grown using various methods

Method	Tip diameter (nm)	Structure	Growth rate (nm/min)	Growth temperature (°C)
VHF-PECVD [present research]	<3	Crystalline	500	370
PECVD [22]	<10	Crystalline/amorphous	1000	400
LPCVD [30]	40	Crystalline/amorphous	50	500
PECVD [15]	<30	Crystalline/amorphous	12	380
CVD [24]	50–60	–	50	400–500

instance atomic force microscopy (AFM), due to their low apex angle (<5°). These Si nanowires also would be beneficial for field emission and solar cell applications as good light absorbers [8, 33, 34].

Conclusions

In summary, ultra-sharp pointed tip Si nanowires have been synthesized by VHF-PECVD method using VLS mechanism. Using this method single crystalline ultra-sharped SiNWs were fabricated with very fast growth rates at low synthesis temperatures. These needle-like wires are used in nanodevices.

References

1. Morales AM, Lieber CM (1998) Science 279:208
2. Cao L, Park JS, Fan P, Clemens B, Brongersma ML (2010) Nano Lett 10(4):1229
3. Cao L, Fan P, Barnard ES, Brown AM, Brongersma ML (2010) Nano Lett 10(7):2649
4. Shan Y, Fonash SJ (2008) ACS Nano 2(3):429
5. Najmzadeh M, Michielis LD, Bouvet D, Dobrosz P, Olsen S, Ionescu AM (2010) Microelectron Eng 87:1561
6. Wanekaya AK, Chen W, Myung NV, Mulchandani A (2006) Electroanalysis 18(6):533
7. Li Q, Koo SM, Edelstein MD, Suehle JS, Richter CA (2007) Nanotechnology 18:315202 (5 pp)
8. Kelzenberg MD, Turner-Evans DB, Kayes BM, Filler MA, Putnam MC, Lewis NS, Atwater HA (2008) Nano Lett 8(2):710
9. Olinga TE, Frayasse J, Travers JP, Dufresne A, Pron A (2000) Macromolecules 33:2107
10. Zhang YF, Tang YH, Wang N, Yu DP, Lee CS, Bello I, Lee ST (1998) Appl Phys Lett 72:1835
11. Holmes JD, Johnston KP, Doty RC, Korgel BA (2000) Science 287:1471
12. Zhang YF, Tang YH, Lam C, Wang N, Lee CS, Bello I, Lee ST (2000) J Cryst Growth 212:115
13. Peng K, Xu Y, Wu Y, Yan Y, Lee ST, Zhu J (2005) Small 1:1062
14. Wu Y, Chi Y, Huynh L, Barrelet CJ, Bell DC, Lieber CM (2004) Nano Lett 4:433
15. Hofmann S, Ducati C, Neill RJ, Piscanec S, Ferrari AC, Geng J, Dunin-Borkowski RE, Robertson J (2003) J Appl Phys 94(9): 6005
16. Wagner RS, Ellis WC (1964) Appl Phys Lett 4:89
17. Paulo AS, Arellano N, He R, Carraro C, Maboudian R, Howe R, Bokor J, Yang P (2007) Nano Lett 7:1100
18. Shah A, Meier J, Vallat-Sauvain E, Wyrsch N, Kroll U, Droz S, Graf U (2005) Sol Energy Mater Sol Cells 78:469
19. Takatsuka H, Noda M, Yonekura Y, Takeuchi Y, Yamauchi Y (2004) Sol Energy 77:951
20. Gentile P, David T, Dhalluin F, Buttard D, Pauc N, Hertog MD, Ferret P, Baron T (2008) Nanotechnology 19:125608
21. Niu JJ, Wang JN (2008) Mater Lett 62:767
22. Červenka J, Ledinský M, Stuchlíková H, Stuchlík J, Výborný Z, Holovský J, Hruška K, Fejfar A, Kočka J (2010) Phys Status Solidi RRL 4(1–2):37
23. Cui Y, Lauhon LJ, Gudiksen MS, Wang J, Lieber CM (2001) Appl Phys Lett 78:2214
24. Salhi B, Grandidier B, Boukherroub R (2006) J Electroceram 16:15
25. Jeon M, Kamisako K (2009) Met Mater Int 15:83
26. Woo RL, Gao L, Goel N, Hudait MK, Wang KL, Kodambaka S, Hicks RF (2009) Nano Lett 9(6):2207
27. Adu KW, Gutierrez HR, Eklund PC (2006) Vib Spectrosc 42:165
28. Yu DP, Bai ZG, Ding Y, Hang QL, Zhang HZ, Wang JJ, Zou YH, Qian W, Xiong GC, Zhou HT, Feng SQ (1998) Appl Phys Lett 72:3458
29. Adu KW, Guti'errez HR, Kim UJ, Sumanasekera GU, Eklund PC (2005) Nano Lett 5:409
30. Lugstein A, Hyun YJ, Steinmair M, Dielacher B, Hauer G, Bertagnolli E (2008) Nanotechnology 19:485606
31. Becker M, Sivakov V, Gösele U, Stelzner T, Andrä G, Reich HJ, Hoffmann S, Michler J, Christiansen SH (2008) Small 4:398
32. Kikkawa J, Ohno Y, Takeda S (2005) Appl Phys Lett 86:739
33. Au CK, Wong KW, Tang YH, Zhang YF, Bello I, Lee ST (1999) Appl Phys Lett 75:1700
34. Chuen YL, Chou LJ, Hsu CM, Kung SC (2005) J Phys Chem B 109:21831